ELSEVIER

Polymer 40 (1999) 283–288

polymer

X-ray absorption spectroscopy studies of zinc-neutralized ethylene-methacrylic acid ionomers

Brian P. Grady[a,*], Jill A. Floyd[a], W. Berlin Genetti[a], Pierre Vanhoorne[b,†], Richard A. Register[b]

[a]*School of Chemical Engineering and Materials Science, University of Oklahoma, Norman, OK 73019-0628, USA*
[b]*Department of Chemical Engineering, Princeton University, Princeton, NJ 08544-5263, USA*

Received 2 April 1997; revised 7 February 1998; accepted 13 March 1998

Abstract

A series of zinc-neutralized ethylene-methacrylic acid ionomers was studied using X-ray absorption spectroscopy. Neutralization methodology, neutralization level and methacrylic acid content were varied to test whether any of these factors affected the local environment of the zinc cations. Three different neutralization methods were tested: melt neutralization with zinc oxide, melt neutralization with zinc acetate and solution neutralization with zinc acetate. Neutralization levels varied between 25 and 100% of stoichiometric, and methacrylic acid contents varied between 10 and 20% by weight. Samples were prepared and handled to rigorously exclude water. Despite the substantial differences in sample preparation procedures, the local environments around the zinc atoms were identical in all materials, resembling the arrangement of atoms in the crystal structure of monoclinic anhydrous zinc acetate. In this compound, four oxygen atoms surround the zinc atom with distances ranging from 1.950 to 1.965 Å.

Keywords: Ionomer; EXAFS; Ethylene-methacrylic acid

1. Introduction

The remarkable improvement in mechanical properties of polymers having a small fraction of ionic groups covalently bonded to the polymer backbone is due to phase separation of the ionic groups into nanometre-size ionic-rich aggregates. The aggregates act as both reinforcing filler and crosslinks, leading to improvement in such properties as mechanical strength, abrasion and tear resistance, and impact strength [1] as well as profoundly affecting the rheological properties [2]. The extent to which these ionic associations modify properties depends on the strength of ionic association, which can be reflected in the local structure inside the aggregates [3]. The fundamental reason for phase separation is the favourable energetics of ionic group association.

This study examines the atomic-scale internal structure of the aggregates in zinc-neutralized ethylene-methacrylic acid (E-MAA) ionomers. This type of ionomer is marketed by DuPont under the trademark Surlyn®. Neutralization with zinc is preferred in many packaging applications, as the zinc-neutralized ionomers have better adhesion in coextrusion and foil coating [4]. However, while neutralization of E-MAA with alkali metals (typically using the hydroxide) is straightforward, the amphoteric nature of zinc makes its use as a neutralizing agent more complicated. The melt neutralization process used to produce Surlyn® ionomers is very different than the solution neutralization process often employed in a laboratory. This difference in neutralization procedure could lead to other differences; for example, unreacted neutralizing salt might remain in the commercial ionomer since the industrial process relies on mechanical mixing to overcome possible cation transport limitations. Also, commercial E-MAA ionomers are typically not stoichiometrically neutralized with a metal cation, i.e. typically acid groups are present even if all the added salt participates in the neutralization. The effect of acid groups on the internal aggregate structure is not well documented. To help answer these questions, we employ extended X-ray absorption fine structure (EXAFS) to determine the structure around the zinc neutralizing cation. Previous studies of ionomers have shown that EXAFS can detect structural differences which underlay property differences; for example, large changes in melt viscosity [5] and dynamic mechanical properties [6] which are seen upon plasticizing zinc sulfonated polystyrene with glycerol are reflected in the cation local structure as measured by EXAFS [7].

EXAFS is the measure of oscillations in the X-ray

* Corresponding author.
† Present address: Bayer AG, D-51368 Leverkusen, Germany.

0032-3861/98/$ - see front matter
PII: S0032-3861(98)00239-0

absorption coefficient on the high-energy side of an absorption edge. An absorption edge occurs when the energy of the X-ray is just sufficient to cause the ejection of an electron from an atom in the material. Oscillations occur owing to interference between the outgoing photoelectron waves and photoelectron waves backscattered by nearby atoms. The shape and period of the oscillations are functions of the absorbing atom (in this paper, zinc) as well as the type, distance and number of atoms around the absorbing atom. Hence, EXAFS offers a means to probe the local atomic arrangement of materials. The maximum distance probed by this technique is 5–6 Å; in ionomers information is typically limited to nearest and next-nearest neighbours of the absorbing atom because of the low atomic number atoms and hence weak backscatterers found in polymers. The information from EXAFS is similar to that available from more common wide-angle X-ray diffraction; however, long-range translational symmetry is not required for EXAFS. Further information about the theoretical basis of EXAFS can be found in previous publications by the authors [8,9] and a treatise on the subject [10].

Normally, the EXAFS region is considered to be ≈ 40 eV above the edge and beyond. The technique concerned with variations in the X-ray absorption coefficient closer to the edge is termed X-ray absorption near-edge spectroscopy (XANES). Together, these two measurements are termed X-ray absorption spectroscopy (XAS). Theory for XANES spectral interpretation is not as well developed as that for EXAFS interpretation, since factors other than the local atomic structure influence XANES spectra. These factors include the charge density state in the atom, multiple electron excitations and Rydberg state absorption (instead of fully ionizing the electron, the electron undergoes a transition from one electronic state to another) [11]. The important structural information available in the XANES region is due to scattering paths where the electron must travel a long distance. Multiple scattering is the most common event causing features in the XANES region; however, in carboxylate ionomers it is possible that the closest metal cations might contribute to XANES features because metals are such strong backscatterers compared with oxygen and carbon.

The purpose of this study is to measure XAS spectra of different zinc carboxylated ionomers in order to quantify the local environment around the zinc atom in dry ionomers. Four other similar studies involving zinc carboxylate ionomers have appeared in the literature [3,12–14]. Three of these studies [3,12,13] concluded that zinc was four-fold coordinated to oxygen at a distance of approximately 1.96 Å, which agrees with the findings in this study. The latter of the three studies examined carboxy-telechelic butadiene (CTB); the findings in this study differed from those in an earlier EXAFS study [14] of zinc-neutralized CTB by the same authors. The major experimental difference between the two studies was the neutralizing agent; diethyl zinc was used in the earlier study while zinc acetate was used in the later study. The study presented in this paper examines the effect of neutralization procedure on the cation local structure in zinc E-MAA ionomers. In addition, the effects of methacrylic acid comonomer content and the presence or absence of unneutralized acid groups are examined.

2. Experimental

A total of 11 samples were tested and labelled as the following: @##-##. The first letter represents the neutralization method, either solution neutralization with zinc acetate dihydrate (S), melt blending with zinc oxide on a laboratory mill (L), or melt blending with zinc oxide on an industrial mill (I). The first two numbers represent the nominal methacrylic acid content in weight percent, while the second pair of numbers represents the percentage of methacrylic acid residues neutralized as determined by infrared spectroscopy. Thus L11-29 represents a sample neutralized on a laboratory mill with 11 weight percent methacrylic acid content and 29 percent neutralized with zinc. Two samples, L11-29a and S11-54e, have an extra character; the letter 'a' indicates that melt neutralization was performed with zinc acetate rather than zinc oxide, while 'e' represents an ionomer in which unneutralized acid groups were converted to the methyl ester. All melt-neutralized samples were provided in pelletized form by DuPont. Descriptions of the solution neutralization and esterification methods are given in a recent publication [15].

All melt-neutralized samples were dried for 1 week in a vacuum oven at 70°C, then compression moulded at 700 bar into 32 mm discs. The thickness of all samples was adjusted so that the absorbance was approximately 2 at 100 eV above the edge. Finished samples were then dried in a vacuum oven for approximately another week at 70°C and then transferred into a special shipping liquid nitrogen dewar for transport to the Stanford Synchrotron Research Laboratory (SSRL). Solution neutralized samples were compression moulded into 28 mm discs as described in a previous paper [15] and then dried for 2 weeks at 70°C in a vacuum oven before shipment.

XAS spectra from the ionomers were compared with the XAS spectrum of anhydrous zinc acetate. Anhydrous zinc acetate powder was obtained from the Aldrich Chemical Company then dried for one week in a vacuum oven at 50°C. Samples for XAS were made by dispersing the powder on polyimide tape inside a glove box, then quickly placing the samples into the shipping dewar. Zinc oxide and zinc hydroxide obtained from Aldrich were also prepared similarly and measured.

XAS measurements were made at SSRL on Beamline 2-3 using a Si(111) monochromator. 5 eV steps were used in the pre-edge and EXAPS regions, while 1 eV steps were used from 16 eV below the edge to 40 eV above the edge. 0.7 mm entrance slits were used to obtain high energy

resolution; further reduction in entrance slit width would not have improved the energy resolution for this beamline and energy [16]. Energy calibration was performed with zinc foil. The incoming and outgoing X-ray intensities were monitored using nitrogen-filled 15 and 30 cm ionization chambers, respectively. A third chamber of 30 cm length was placed after the second chamber and zinc foil was mounted between the second and third chambers to provide an energy reference for all samples. Five to seven scans (each lasting approximately 20 min) were collected and added together after edge energy determination before further analysis to improve the signal to noise ratio. XAS spectra were measured with the samples at room temperature and at 20 K. For room temperature scans, the samples were mounted in a specially designed box which maintained the samples under positive nitrogen pressure. For 20 K scans, the samples were mounted in an Oxford Instruments continuous flow liquid helium cryostat. The data presented in this paper represent results from experiments carried out at two different times on the same beamline.

AUTOBK [17], a commercial software package available from the University of Washington UWXAFS project, was used to convert the measured absorbance versus X-ray energy (E) curves to $k^2\chi(k)$ versus k according to the formula below:

$$\chi(k) = \frac{\mu(E) - \mu_0(E)}{\mu_0(E)} \quad (1)$$

where $\mu(E)$ and $\mu_0(E)$ are the measured and mean absorption coefficients, respectively, at energy E. k is termed the wavevector and is given by:

$$k = \sqrt{\frac{2m_e}{\hbar^2}(E - E_0)} \quad (2)$$

where E_0 is the absorption edge energy, m_e is the mass of an electron and $\hbar$ is Planck's constant divided by 2π. A representative $k^2\chi(k)$ versus k spectrum for an ionomer is shown in Fig. 1.

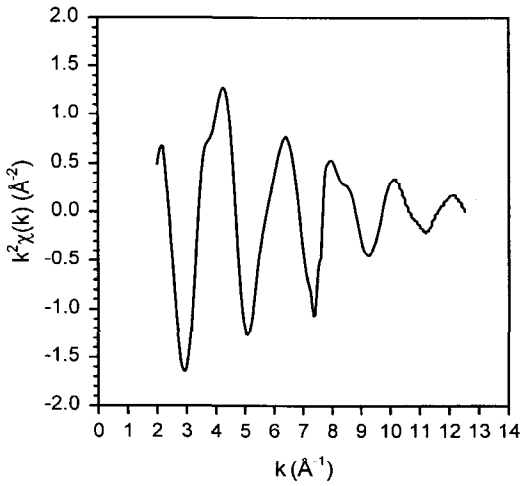

Fig. 1. A plot of $k^2\chi(k)$ *versus* k for a representative ionomer sample (L11-29) at 20 K. Fourier transformation of this data yields the radial structure function shown in Figs 2 and 3.

After isolation of the EXAFS oscillations and truncation of the spectra to the region $k = 2$–12.5 Å^{-1}, the data were Fourier transformed to obtain the radial structure function (RSF). The radial structure function is similar to a radial distribution function in that peaks in the RSF usually correspond to distinct coordination shells. The abscissa of the RSF has units of Å, but the locations of peaks are shifted from the true interatomic distances, hence a subscript F will be used to distinguish this distance from the actual interatomic distance R. Fitting of the data to model structures was performed using FEFFIT from UWXAFS in combination with FEFF6 [18] allowing the mean squared displacement for the first coordination shell and the edge energy to vary. Mean squared displacements for higher shells were fixed at 0.005 Å^2. The mean squared displacement quantifies the variation in distance between the absorbing atom and atoms in a single coordination shell, and includes contributions due to static variations (two atoms may be at slightly different distances but are considered to be in the same coordination shell) and thermal vibrations.

Excitations of electrons other than the ejected electron reduce the amplitude of the EXAFS oscillations relative to the absorption increase at the absorption edge. This effect is quantified through the amplitude reduction parameter, S_0^2, which should be identical for all samples in this experiment. S_0^2 is a constant by which the theoretical RSF must be multiplied in order to obtain a good representation of the experimental RSF. The amplitude reduction parameter is difficult to predict from first principles and is best determined by analysis of small-molecule standards with known crystal structure, and whose local structure is similar to that of the species of interest. By analysing EXAFS data for anhydrous zinc acetate, zinc oxide and zinc hydroxide, S_0^2 was determined to be 1.0, and this value was used in the modelling.

3. Results and discussion

Zinc carboxylate ionomers have at least four possible small molecule analogues. Anhydrous zinc acetate has two crystalline structures, an orthorhombic form [19] and a monoclinic form [20]. Zinc acetate also exists commonly as a dihydrate. Another compound, zinc oxyacetate [21], $Zn_4O(CH_3COO)_6$, is a fourth possibility. Fig. 2 shows the radial structure function (solid line) for the ionomer L11-29, obtained by Fourier transformation of the data in Fig. 1. Model fits to the data, discussed in more detail below, indicate that the distance of the oxygen nearest neighbour is approximately 1.96 Å consistent with zinc fourfold coordinated to oxygen [22]. The dihydrate, which has six oxygens coordinated to zinc, is thus eliminated as a possibility. The best-fit spectra for the other three alternatives are shown as dashed lines in Fig. 2; arrangements of atoms are based on

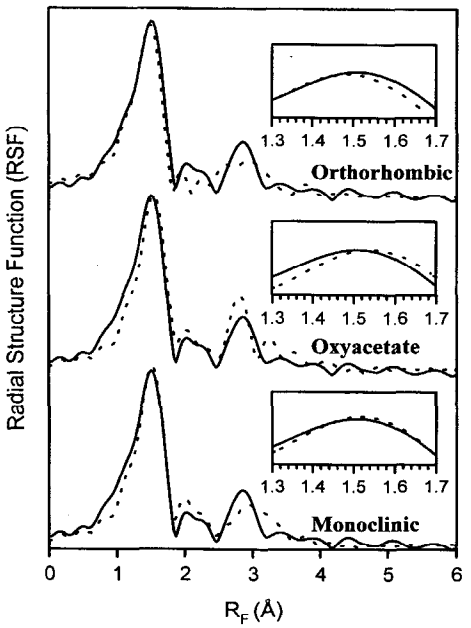

Fig. 2. Comparison of best fit structure (dashed lines) to representative ionomer sample (L11-29) at 20 K using the crystal structures of monoclinic anhydrous zinc acetate, orthorhombic zinc acetate and zinc oxyacetate. Data have been shifted vertically to improve presentation quality. Mean squared displacements were allowed to vary for the first coordination shell, which consists of four oxygen atoms; the mean squared displacements for all other atoms were set to 0.005 $Å^2$.

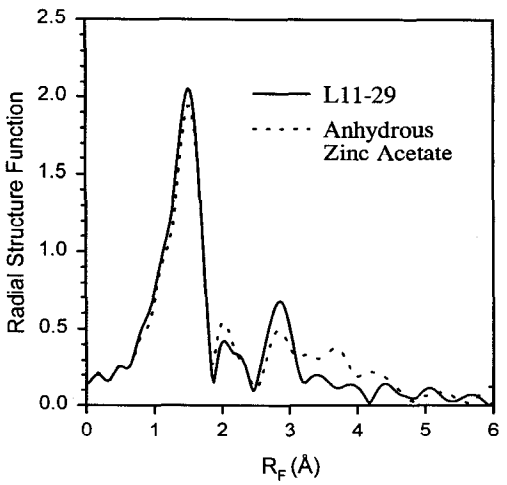

Fig. 3. Experimental radial structure function of representative 20 K ionomer sample (L11-29) at 20 K compared with experimental radial structure function of anhydrous zinc acetate at 20 K.

the published crystal structures. Qualitative differences in the radial structure functions at R_F between 2 and 4 Å as well as differences in location of the peak positions at $R_F \approx 1.5$ Å eliminate the orthorhombic form. The mismatch in peak positions at $R_F \approx 1.5$ Å suggests that the position of atoms inside the aggregate is not that of the oxyacetate either. Further, zinc oxyacetate forms via vacuum distillation of the anhydrous acetate at 250°C and 0.2 mm at roughly 50% yield. Mixing acetic acid with zinc oxide in

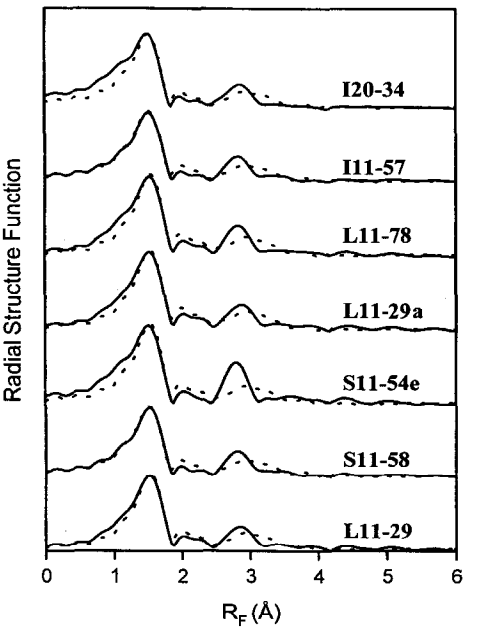

Fig. 4. Radial structure functions for several ionomers obtained at 20 K. Data have been shifted vertically to improve presentation quality. For each ionomer, the solid line represents the experimental data and the dashed line represents the best fit corresponding to the mean squared displacements for the zinc–oxygen first coordination shell listed in Table 1. All other mean squared displacements were set to 0.005 $Å^2$.

a water/toluene mixture, boiling off the water, and then continuing to stir and heat the mixture does not form the oxyacetate [23]. Since solution neutralization of the ionomer is very similar to the latter procedure, it is not surprising that the local structure in the ionomer does not closely resemble that of the oxyacetate.

Fig. 3 shows a direct comparison between the experimental radial structure functions of the monoclinic anhydrous zinc acetate and the ionomer. X-ray diffraction measurements of the anhydrous zinc acetate powder were generally consistent with the published monoclinic structure [20] and wholly inconsistent with the orthorhombic structure [19]. Fig. 3 indicates that the number and position of the first shell oxygen atoms are identical within experimental error for the powder and the ionomer. The differences between the ionomer and the zinc acetate powder in the range 2.5 Å $< R_F <$ 3.2 Å indicate that the similarity between the two breaks down in the higher coordination shells. This disagreement is not surprising because the cations in the ionomer do not possess long-range order because of the small diameter of the aggregates. Further, the methyl groups in zinc acetate are actually polymer chains in the ionomer, so the two structures cannot be identical beyond the third coordination shell. Nonetheless, the immediate environment of the zinc cations in the ionomer very closely resembles the immediate environment in the monoclinic form of anhydrous zinc acetate.

Due to the large number of ionomers measured, it is not practical to display a radial structure function for each sample. Rather, representative data at 20 K are shown in

Table 1
Mean squared displacements for fits

Ionomer	Mean squared displacement at room temperature ($Å^2$)	Mean squared displacement ($Å^2$) at 20 K ($Å^2$)
I12-38	0.0044	0.0037
I20-34	0.0045	0.0029
S11-58	0.0047	0.0035
S11-54e	0.0039	0.0026
I11-57		0.0036
L11-29		0.0032
L11-55		0.0030
L11-68		0.0031
L11-78		0.0029
L11-29		0.0030
L11-26		0.0029

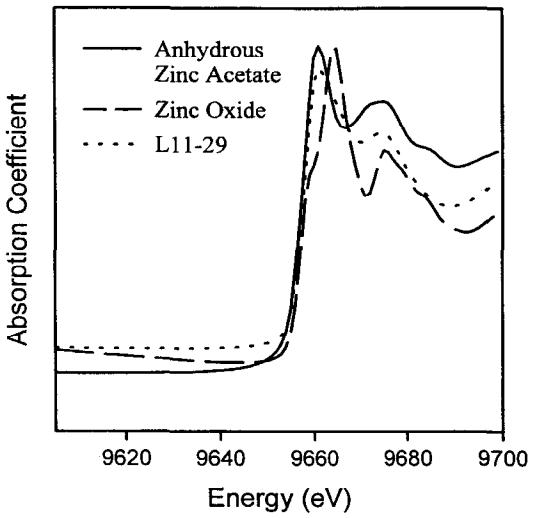

Fig. 5. XANES spectra taken at 20 K comparing a representative ionomer (L11-29) with anhydrous zinc acetate and zinc oxide. The energy scale was adjusted for each sample to the same zinc foil edge energy. Note the similarity between the ionomer and acetate spectra.

Fig. 4, along with the best-fit theoretical RSFs. The samples for which data are presented in Fig. 4 span a factor of two in methacrylic acid content, a factor of nearly four in neutralizing level, have unneutralized acid groups present or absent, and represent four different neutralization methodologies. Despite these differences, the experimental radial structure functions are very similar. Spectra do have small variations in peak height primarily at $R_F \approx 2.8$ Å. These differences might represent changes in the local aggregate structure; however, it is believed these minor variations are within experimental uncertainty.

Table 1 shows the best-fit mean squared displacement for the zinc–oxygen first coordination shell. Differences between spectra measured on the same sample at the two different temperatures were limited to differences in peak heights and widths. The average of mean squared displacements for samples measured at room temperature was 0.0045 $Å^2$ while the average for samples measured at 20 K was 0.0032 $Å^2$. This difference was due to the fact that the thermal vibrations of atoms increase as the temperature increases and hence the mean squared displacements will also increase. Both the data acquired at room temperature and at 20 K have a standard deviation in the best-fit mean squared displacements of 0.0003 $Å^2$. The correspondence between standard deviations at the two temperatures and the small magnitude are extremely gratifying since the standard deviation should reflect only measurement error and modelling uncertainty, neither of which should depend significantly on temperature.

Two further observations can be made based on the RSFs shown in Fig. 4 and data displayed in Table 1:

(1) In agreement with conclusions drawn from rheological and infrared spectroscopic data [15], the local environment around zinc in the unesterified and esterified materials appears identical, indicating that the acid groups commonly found in partially neutralized zinc ionomers do not complex with the cations. Further, Fig. 4 shows that the effect of neutralization level on the internal aggregate structure is either very small or nonexistent If general, the invariance of local environment to neutralization level is probably true only for atoms such as zinc that form strong coordination bonds to the anion atoms. In fact, rheological and infrared spectroscopic study of sodium-neutralized E-MAA ionomers [15] demonstrates that acid groups interact significantly with the aggregates, and presumably EXAFS studies would show that neutralization level changes the local structure around the sodium cation. Since all measurements in this study were conducted at or below room temperature, it is possible the local structure could be different in the melt; an infrared spectroscopic study found that E-MAA groups and zinc cations mixed inside aggregates at temperatures above 100°C to form acid salts [24]. However, a more recent study suggests that changes in the infrared spectra that led to this assignment may have been due to water absorption [25].

(2) The neutralization methods and drying regimens described in this paper produce ionomers having the same local aggregate structure. This statement does not imply that the neutralization method is unimportant, since some solution neutralization procedures attempted did not convert the carboxylic acid groups to salt. Further, the water contents of the ionomers prior to vacuum drying were likely different for the different neutralization protocols; the identical local structure revealed by EXAFS demonstrate the effectiveness of the vacuum drying procedure. Finally, this conclusion implies no neutralizing agent contamination by zinc oxide. If a significant amount of unreacted zinc oxide were present in the I- or L-series ionomers, the peak at $R_F \approx 2.8$ would be much larger since the EXAFS spectrum for zinc oxide has a large peak at this distance [8].

XANES spectra of the ionomers are essentially identical at a given temperature, similar to the agreement shown for

radial structure functions. Using data from the third ionization chamber, the energy scales for all XANES spectra were adjusted to be consistent. A representative ionomer spectrum at 20 K is shown in Fig. 5 along with the XANES spectra of anhydrous zinc acetate and zinc oxide. The general shape of the spectra for the ionomer and anhydrous zinc acetate agree, although larger differences exist between these two XANES spectra than exist between any two ionomer XANES spectra. The XANES spectra in Fig. 5 demonstrate that substantial quantities of zinc oxide, the neutralizing agent used in the preparation of L11-29, do not remain in the final ionomer. This conclusion is further supported by the close similarity of the XANES spectra obtained from ionomers in the L- and I-series (neutralized with zinc oxide) and from ionomers in the S-series and L11-29a (neutralized with zinc acetate).

4. Summary

The excellent agreement between model and experiment for the zinc ionomer samples supports the conclusion proposed in a previous study of cadmium ionomers [9]: the local environment around the neutralizing cation is similar to that found in the crystal structure of the small molecule analogue. Steps were taken to rigorously exclude water from these samples, since water will preferentially migrate to the ionic domains and presumably significantly alter the local environment around the cation significantly. The next step in this series of experiments will be to examine more closely the effect of water and other plasticizers on the X-ray absorption spectra of these ionomers.

Acknowledgements

Melt-neutralized E-MAA was kindly supplied by Dr. John Paul of the DuPont Sabine Research Laboratory; the authors also acknowledge Dr. Paul for his many stimulating technical discussions. The authors would like to thank Ms. Sangamithra Chintapalli for her help in running the XAS experiments at SSRL as well as the SSRL staff, in particular Ingrid Pickering, Sean Brennan and Britt Hedman. Financial support for this project was provided by the DuPont Sabine Research Laboratory, NSF EPSCoR for BPG and WBG (Cooperative Agreement No OST-9550478) and a NATO Postdoctoral Fellowship (PVH). SSRL is operated by the Department of Energy; Office of Basic Energy Sciences. The SSRL Biotechnology Program is supported by the NIH, Biomedical Research Technology Program, National Center for Research Resources. Further support for SSRL is provided by the Department of Energy, Office of Health and Environmental Research.

References

[1] Eisenberg A, King M, editors. Ion containing polymers. New York: Haisted-Wiley, 1975.
[2] Register RA, Prud'homme RK. Melt rheology. In: Tant MR, Mauritz KA, Wilkes GL, editors. Ionomers: synthesis, structure, properties and applications. New York: Blackie, 1997.
[3] Register RA, Foucart M, Jerome R, Ding YS, Cooper SL. Macromolecules 1988;21:1009. Register RA, Foucart M, Jerome R, Ding YS, Cooper SL. Macromolecules 1988;21:2652.
[4] Longworth R, Nagel H. Packaging. In: Tant MR, Mauritz KA, Wilkes GL, editors. Ionomers: synthesis, structure, properties and applications. New York: Blackie, 1997.
[5] Lundberg RD, Makowski HS, Westerman L. The dual plasticization of sulfonated polystyrene ionomer. In: Eisenberg A. editor. Ions in polymers, ACS Adv. Chem. Ser. 187. Washington, DC: American Chemical Society, 1980.
[6] Weiss RA, Fitzgerald JJ, Kim D. Macromolecules 1991;24:1064.
[7] Ding YS, Register RA, Nagarajan MR, Pan HK, Cooper SL. J Polym Sci Part B 1988;26:289.
[8] Grady BP, Cooper SL. Macromolecules 1994;27:6627.
[9] Grady BP, Moore RB. Macromolecules 1996;29:1685.
[10] Teo BK. EXAFS: basic principles and data analysis. New York: Springer, 1986.
[11] Bianconi A. XANES spectroscopy. In: Koningsberger DC, Prins R, editors. X-ray absorption, principles, applications, techniques of EXAFS, SEXAFS and XANES. New York: Wiley-Interscience, 1988.
[12] Yarusso DJ, Ding YS, Pan HK, Cooper SL. J Polym Sci Part B 1984;22:2073.
[13] Vlaic G, Williams CE, Jerome R, Tant MR, Wilkes GL. Polymer 1988;29:173.
[14] Jerome R, Vlaic G, Williams CE. J Phys Lett 1983;44:L717.
[15] Vanhoorne P, Register RA. Macromolecules 1996;29:598.
[16] Hedman B, Stanford Synchrotron Radiation Laboratory, personal communication.
[17] Newville M, Līviņš P, Yacoby Y, Rehr JJ, Stern EA. Phys Rev B 1993;47:14126.
[18] Zabinsky SI, Rehr JJ, Ankudinov A, Albers RC, Eller MJ. Phys Rev B 1995;52:2995.
[19] Capilia A, Aranda A. Cryst Struct Commun 1979;8:705.
[20] Clegg W, Little IR, Straughan BP. Acta Crystallogr 1982;C42:1702.
[21] Kayama H, Saito Y. Bull Chem Soc Jpn 1954;27:112.
[22] Pan HK, Knapp GS, Cooper SL. Colloid Polym Sci 1984;262:734.
[23] Gordon RM, Silver HM. Can J Chem 1983;61:1218.
[24] Coleman MM, Lee JY, Painter PC. Macromolecules 1990;23:2339.
[25] Ishioka T. J Polym 1993;25:1147.